BEST BANDS SELECTION FOR DETECTION IN HYPERSPECTRAL PROCESSING

Nirmal Keshava

MIT Lincoln Laboratory
244 Wood Street Lexington, MA 02420-9185
keshava@ll.mit.edu, (o) (781) 981-3344

ABSTRACT

In this paper, we explore the role of best bands algorithms in the context of maximizing the performance of hyperspectral algorithms. Specifically, we first focus on creating an intuitive framework for how metrics quantify the distance between two spectra. Focusing on the Spectral Angle Mapper (SAM) metric, we demonstrate how the separability of two spectra can be increased by choosing the bands that maximize the metric. This intuition about best bands analysis for SAM is extended to the Generalized Likelihood Ratio Test (GLRT) for a practical target/background detection scenario. Results are shown for a scene imaged by the HYDICE sensor demonstrating that the separability of targets and background can be increased by carefully choosing the bands for the test.

1. INTRODUCTION

Hyperspectral data typically consists of radiometric measurements in hundreds of contiguous spectral channels. Collectively, and in their natural order, these bands comprise a vector for each pixel in the scene having a length equal to the number of channels and conveys the emissive and reflective properties of the scene being imaged. Significant attention has been given to using the full length vector for traditional applications such as spectral unmixing and detection with the normal rules applying from the domain of linear algebra. Very little attention, however, has been given to determining whether these applications actually require the full complement of spectral measurements, or whether superior performance can actually be achieved from a limited spectral regime, or perhaps, even from a subset or bands located at arbitrary wavelengths along the full spectrum.

This work was sponsored by the Department of the Defense under Contract F19628-00-C-0002. Opinions, interpretations, conclusions, and recommendations are those of the author and are not necessarily endorsed by the United States Air Force.

1.1. Best Bands Algorithms

Best bands algorithms find the subset of bands in multispectral or hyperspectral data that yield the best performance based on some criteria that is usually linked to some measure of end-performance. They are intrinsically related to metrics, which, essentially *translate* the physical measurements collected at the sensor into numerical quantities suitable for mathematical and statistical modelling[1]. For detection, this measure is commonly expressed in receiver operator characteristic (ROC) curves depicting probabilities of false alarm (P_{FA}) and detection (P_D). For estimation, Cramer-Rao bounds provide confidence measures for estimates, and for classification, probabilities of correct classification (P_{CC}) are used.

The best bands problem has been posed for applications related to multispectral sensing where the bands are neither contiguous nor do they possess spectral resolution equivalent to that of hyperspectral sensors [2]. More importantly, the number of bands is typically less than ten, and solutions derived from algorithms can be verified against an exhaustive test of all possible band combinations. Having hundreds of bands, hyperspectral data poses a more formidable challenge.

2. MAXIMIZING SEPARABILITY

Previously, we have considered best bands analysis in the general context of an arbitrary application whose performance can be optimized by the appropriate selection of hyperspectral bands. In this section, we focus on the specific task of target detection, starting with the simplest examples, and incrementally progressing to a realistic detection scenario.

2.1. Maximizing SAM

Consider the reflectance spectra for two different targets in Figure 1. Clearly, they are visually different in both shape and amplitude. Their similarity can be measured using the Spectral Angle Mapper (SAM), which returns the angle be-

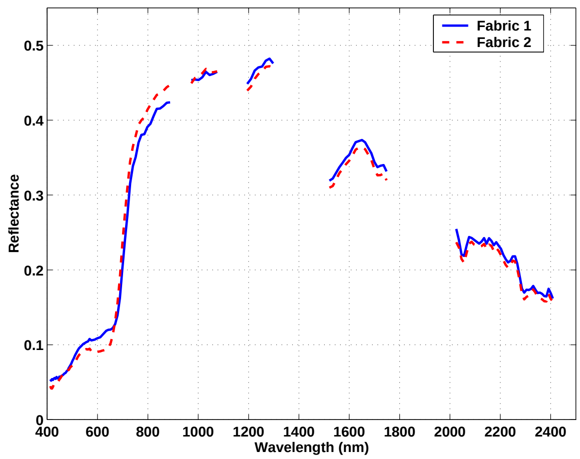

Fig. 1. Spectra for two similar fabrics (bad bands removed).

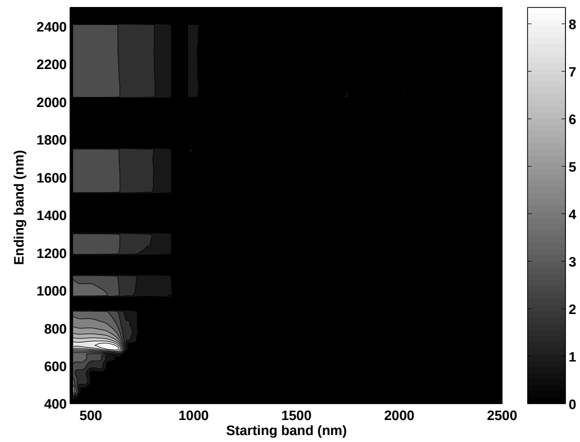

Fig. 2. SAM contour map for two similar fabrics.

tween two vectors of equal length, $\mathbf{x}$ and $\mathbf{y}$:

$$\theta(\mathbf{x},\mathbf{y}) = \arccos\left(\frac{<\mathbf{x},\mathbf{y}>}{\|\mathbf{x}\|\|\mathbf{y}\|}\right), \quad 0 \leq \theta \leq \frac{\pi}{2} \qquad (1)$$

where $< \cdot, \cdot >$ is the dot product operator, and $\| \cdot \|$ is the 2-norm which may be written using the dot product operator as $\sqrt{<\mathbf{z},\mathbf{z}>}$ for a vector, $\mathbf{z}$ [3]. Using the two targets plotted in 1, we find the SAM angle is 18.9^o.

Given the SAM value calculated for the two spectra, our goal is now to maximize the SAM value for the two spectra by choosing the proper set of bands. We do this because target classification performance is enhanced when the difference between two targets is maximized. Each target originally had 210 spectral bands, but because some bands are corrupted by atmospheric absorption bands, they are deleted from the vector signals, leaving 144 remaining bands for processing. The abbreviated spectra in Figure 1 reflect the width and location of these omissions. References to band numbers, however, are made with respect to the original 210-band spectrum. Our goal is to find the subset of 144 bands maximizing θ.

One approach to finding the best bands is to examine the expression in (1), and analytically determine what unconstrained subset of bands maximizes θ. Analytical approaches, however, are difficult, and a very open area of research. Instead, we concentrate on a simpler objective: find the single continuous segment of bands that maximizes θ. That is, find the starting and ending band such that the resulting spectra have the maximum SAM value. If θ is calculated for every acceptable pair of starting and ending bands, the result is a two-dimensional contour map. Figure 2 depicts this for the two spectra in Figure 1.

Both targets are green fabrics, but Fabric 1 is noticeably darker. The SAM value for the full spectra is 2.73^o. Figure 2 illustrates the SAM contour map for these two very similar targets. The maximum value for this SAM contour map is 9.18^o and occurs for a starting and ending band pair of $(43, 55)$ that corresponds to the wavelength interval $[596 \text{ nm}, 697 \text{ nm}]$. The increase in the SAM value from 2.73^o is 6.45^o or 236%. Not so coincidentally, the segment yielding the maximum SAM value coincides with the green-yellow part of the visible electromagnetic spectrum. This difference in reflectance for the two targets in these wavelengths is clearly visible in Figure 1.

3. SAM AND STATISTICAL DETECTORS

In Section 2, we optimized the SAM metric by finding a subset of bands in hyperspectral signals that yielded the maximum angular separation. In spite of the improvements in separability, however, the SAM metric is too simple to implement as a detector in real scenarios. Practical detectors are statistical and are designed to maximize the probability of detection (P_D) while minimizing the probability of false alarm (P_{FA}). Moreover, because the statistics of targets and background are rarely, if ever, known beforehand, detectors often adaptively estimate the necessary parameters from the data it is also processing.

As a matter of fact, the SAM metric has been shown to be an extreme simplification of the most general statistical detector, the Generalized Likelihood Ratio Test (GLRT) [4, 5]. We can consider the binary hypothesis model that tests for the presence or absence of a target, $\mathbf{s}$, amid an unstructured background:

$$H_0 : \mathbf{x} = \mathbf{w}, \qquad (2)$$
$$H_1 : \mathbf{x} = \mathbf{s} + \mathbf{w}, \qquad (3)$$

where $\mathbf{w}$ is a Gaussian interference vector having an unknown distribution, $\mathbf{s}$ is the desired target spectrum, and $\mathbf{x}$ is the received signal. Additionally, the hypothesis test is constructed using N target-free training pixels, $\mathbf{x}(\mathbf{n}), n = 1, \ldots, N$ that are assumed to arise from the same Gaussian distribution as $\mathbf{w}$. It can then be shown that the optimal test, $\mathcal{T}(\mathbf{x})$, for a threshold, η_o, and a received pixel, $\mathbf{x}$, is:

$$\mathcal{T}_{GLRT}(\mathbf{x}) = \frac{|\mathbf{s}^t \overline{\mathbf{\Gamma}}_w^{-1} \mathbf{x}|^2}{(\mathbf{s}^t \overline{\mathbf{\Gamma}}_w^{-1} \mathbf{s})(1 + \mathbf{x}^t \overline{\mathbf{\Gamma}}_w^{-1} \mathbf{x})} \underset{H_0}{\overset{H_1}{\gtrless}} \eta_0, \quad (4)$$

and $\overline{\mathbf{\Gamma}}_w = \sum_{n=1}^{N} (\mathbf{x}(n) - \overline{\mu}_w)(\mathbf{x}(n) - \overline{\mu}_w)^t$ is the unscaled estimate of the interference covariance and $\overline{\mu}_w = \frac{1}{N} \sum_{n=1}^{N} \mathbf{x}(n)$ is the sample mean.

4. BEST BANDS ANALYSIS FOR GLRT

The same assertions we made about finding the best bands in hyperspectral signals in Section 2.1 apply to the GLRT. Consequently, we will search again, using exhaustive methods, for the single continuous segment of bands in the original signal that maximizes the detection of targets amid background vegetation. Before, we simply maximized the angular difference between two targets to achieve our goal. For the GLRT, however, a more sophisticated analysis is necessary.

4.1. GLRT Performance Metrics

Like all statistical detectors, the measure of performance for the GLRT consists of maximizing the P_D and minimizing the P_{FA} using probabilistic distributions for the output values (statistics) of the GLRT when applied to target and background pixels.

Two things prevent us from formulating P_D and P_{FA} values so easily. First, target spectra may not be available in sufficient quantities to yield a reliable estimate of the target statistic density function. Second, P_D and P_{FA} estimates are obtained by integrating the parameterized density functions. Instead of trying to achieve P_D and P_{FA} estimates, we can instead examine the minimum separation of the two sets of statistics by establishing the difference, $\mathbf{W}$, between the target pixel with the lowest detection statistic and the background pixel statistic with the highest value.

$$\mathbf{W} = \min \mathcal{T}(\mathbf{x}_t) - \max \mathcal{T}(\mathbf{x}_b) \quad (5)$$

Admittedly, $\mathbf{W}$ reflects neither the shape of the densities, which is critical to any reliable ROC curve analysis, nor does it bound critical operating parameters like the probability of error. Yet, $\mathbf{W}$ does at least offer a worst-case analysis of the separation from a practical viewpoint. Moreover, it does not attempt to provide the problem with any more structure than it actually has.

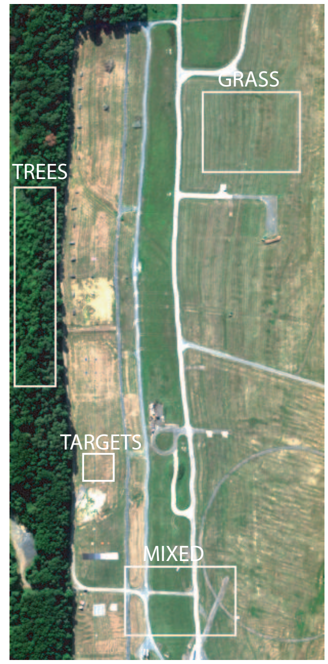

Fig. 3. Forest Radiance I scene.

4.2. Experiment

In Figure 3, the scene imaged for the Forest Radiance I data collection using the HYDICE sensor is shown. Three different target-free regions of background pixels are outlined, as well as one region containing two types of target pixels. For each background region, an estimate of the covariance is determined. GLRT detection results are presented for the case of detecting Target 2 amid trees with the full spectrum. We utilize the same methodology that maximized the SAM metric in Section 2.1 and confine the search to a single continuous segment. The result is a two-dimensional contour map of $\mathbf{W}$, indexed as before by the starting and ending bands.

Figure 4(a) depicts the contour map of $\mathbf{W}$ for the GLRT, where the full spectrum value appears in the upper left-hand corner and the maximum occurs for the band segment $[60, 199]$ (using the numbering from the original 210-band spectrum) , which corresponds to the spectral interval from 752 nm to 2409 nm and is comprised of 88 bands. Background statistic histograms are shown in Figure 4(b) for 8232 pixels using this band interval and the full spectrum. Finally, Figure 4(c) shows the target statistics for 10 pixels. The relevant values for calculating $\mathbf{W}$ have been summarized in Table 1. The increase in $\mathbf{W}$ of 0.099 was due to a dramatic increase in the minimum target statistic.

	Target GLRT stats.		Background GLRT stats.		**W**
	Min.	Max.	Min.	Max.	
Full spec.	.169	.797	.000	.008	**.161**
Best bands	.230	.731	.000	.008	**.221**

Table 1. GLRT statistics for full spectrum and best bands processing.

5. SUMMARY AND FUTURE WORK

We focused on the SAM metric and demonstrated how the angle between the spectra of two objects can be maximized to increase the angular distance by choosing an appropriate set of spectral bands. We then adapted this algorithm to find the bands that optimize a measure of detection performance, which was chosen to be a worst-case measure of target and background separability. Improvement in separability was demonstrated for a target and background combination.

Future work will focus on developing fast methods for optimal band selection that avoid the constraints in the selection process utilized here. In particular, the utility of angle-based measures to compare the similarity of two spectra will be explored. Future results will demonstrate methods of integrating the geometric interpretation of spectra with physics-based justifications.

6. REFERENCES

[1] Nirmal Keshava and Peter Boettcher, "On the relationships between physical phenomena, distance metrics, and best band selection in hyperspectral processing," in *Algorithms for Multispectral, Hyperspectral, and Ultraspectral Imagery VII*, Apr. 2001, vol. 4381 of *Proceedings of the SPIE*.

[2] Charles Sheffield, "Selecting band combinations from multispectral data," *Photogrammetric Engineering and Remote Sensing*, vol. 51, no. 6, pp. 681–687, June 1985.

[3] Gene H. Golub and Charles F. Van Loan, *Matrix Computations*, The Johns Hopkins University Press, 1996.

[4] E. J. Kelly, "An adaptive detection algorithm," *IEEE Trans. Aerospace and Elec. Sys.*, vol. 22, no. 5, pp. 115–127, Mar. 1986.

[5] Dimitris Manolakis, Gary Shaw, and Nirmal Keshava, "Comparative analysis of hyperspectral adaptive matched filter detectors," in *Algorithms for Multispectral, Hyperspectral, and Ultraspectral Imagery VI*, Apr. 2000, vol. 4049 of *Proceedings of the SPIE*, pp. 2–17.

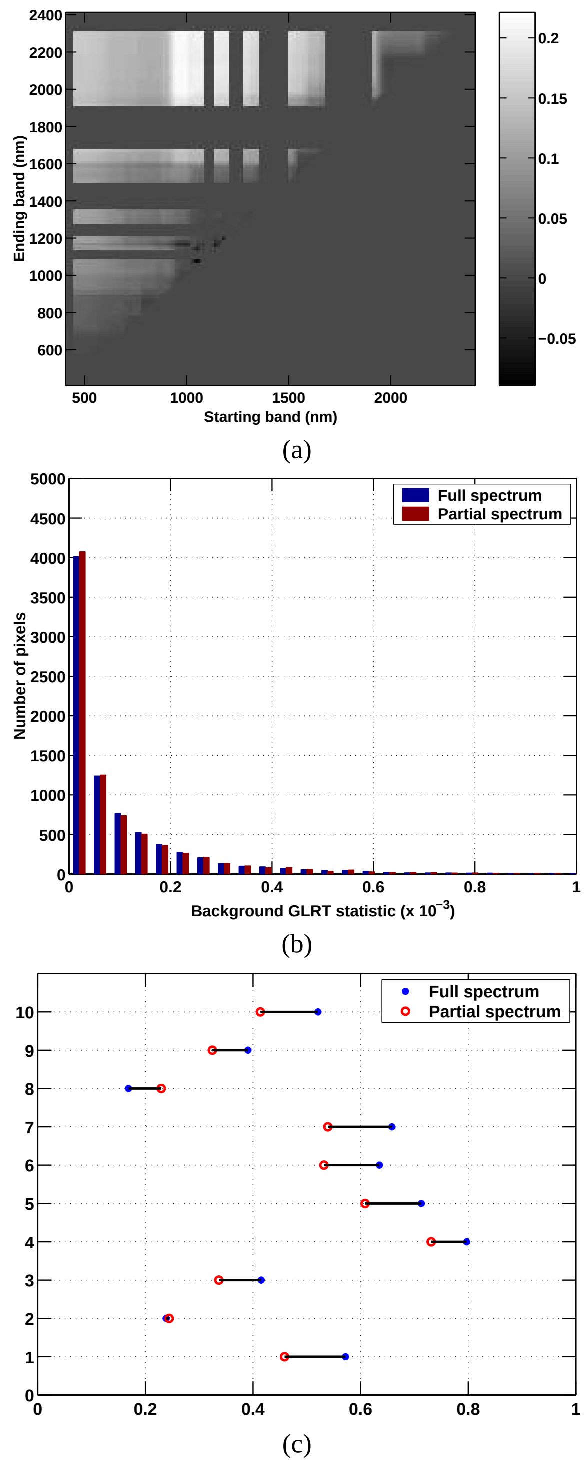

Fig. 4. Target 2 and trees: (a) Contour map for **W**, (b) Background statistic histogram, (c) Target pixel statistics.